2) Further metal purification work on vacuum distillation, centrifugal slagging, and zone refining with alloys of lunar or asteroidal compositions.

3)Deployment of a small scale, Earth-proven system in low Earth orbit to investigate the effect of zero gravity on the process and equipment.

References

[1]Adler, I. et al., "Apollo 15 Geochemical X-Ray Fluorescence Experiment: Preliminary Report," *Science*, Vol. 175, Jan. 1972, pp. 436-440.

[2]Metzger, A., Trombka, J., Reedy, R., and Arnold, J., "Elemental Concentrations from Lunar Orbital Gamma-ray Measurements," *Proceedings of the 5th Lunar Science Conference*, 1974, pp. 1067-1078.

[3]Pieters, C., Gaffey, M. J., Chapman, C. R., and McCord, T. B., "Spectrophotometry of Eros 433 and Compositional Implications," *Icarus*, Vol. 28, 1976, pp. 105-115.

[4]Larson, H. P., Fink, U., Treffersm, R. R., and Gautier, T. N., "The Infrared Spectrum of Asteroid 433 Eros," *Icarus*, Vol. 28, 1976, pp. 95-103.

[5]Veeder, G. J., Matson, D. L., Bergstrahh, J. T., and Johnson, T. V., "Photometry of 433 Eros from 1.65 to 2.2 um," *Icarus*, Vol. 28, 1976, pp. 79-85.

[6]Wisniewski, W. Z., "Spectrophotometry and UBVRI Photometry of Eros," *Icarus*, Vol. 28, 1976, pp. 87-90.

[7]Steurer, W. H., "Lunar Oxygen Production by Vapor Phase Pyrolysis," *Proceedings of the 7th Princeton Conference on Space Manufacturing*, Princeton, NJ, 1985, pp. 123-131.

[8]Rosenberg, D. S., Guter, G. A., and Miller, F. E., "Manufacturing of Oxygen from Lunar Materials," *Annals of the New York Academy of Science*, Vol. 123, July 1965, pp. 1106-1122.

[9]Khalafalla, S. E. and Haas, L. A., "Carbothermal Reduction of Silicous Minerals in Vacuum," *High Temperature Science*, Vol. 2, June 1970, pp. 95-109.

[10]Phinney, W. C., Criswell, D., Drexler, E., and Garmrian, J., "Lunar Resources and Their Utilization," *Progress in Astronautics and Aeronautics: Space-Based Manufacturing from Non-Terrestrial Materials*, edited by M. Summerfield, G. K. O'Neill, and B. O'Leary, AIAA, New York, 1976, pp. 97-123.

[11]Koelle, H. H., "Preliminary Analysis of a Baseline System Model for Lunar Manufacturing," *Acta Astronautical*, Vol. 9, No. 6-7, 1982, pp. 401-413.

[12]O'Leary, B., "Mining the Apollo and Amor Asteroids," *Science*, Vol. 127, 1977, pp. 363-366.

[13]Gaffey, M. J. and McCord, T. B. "Mining Outer Space," *Technology Review*, June 1977, pp. 51-59.

[14]Benton, A. F. and Drake, L. C., "The Dissociation Pressure of Silver Oxide Below 200°," *Journal of the American Chemistry Society*, Vol. 54, 1932. pp. 2186-2194.

[15]Lewis, G. N., "Concerning Silver Oxide and Silver Suboxide," *Journal of the American Chemistry Society*, Vol. 28, 1906, pp. 139-158.

[16]Keyes, F. G. and Hara, H., "The Pressure of Oxygen in Equilibrium With Silver Oxide," *Journal of the American Chemistry Society*, Vol. 44, 1922, pp. 479-485.

[17]Taylor, G. B. and Hulett, G. A., "The Dissociation of Mercuric Oxide," *Journal of Physical Chemistry*, Vol. 17, 1913, pp. 565-591.

[18]Johnson, F. S., *Satellite Environment Handbook*, 2nd ed., Stanford University Press, Stanford, CA, 1965, p. 11.

[19]Roberts, R. W. and Vanderslice, T. A., *Ultrahigh Vacuum and its Application*, Prentice-Hall, Englewood Cliffs, NJ, 1963, pp. 179-185.

[20]Wicks, C. E. and Blocks, F. E., *Thermodynamic Properties of 65 Elements – Their Oxides, Halides, Carbides, and Nitrides*, Bulletin 605, U. S. Bureau of Mines, 1963.

[21]Drowart, J., *Condensation and Evaporation of Solids*, edited by E. Rutner, P. Goldfinger, and J. P. Hirth, Gordon and Breach Science Publishers, New York, 1964, p. 255.

[22]Hass, G., "Preparation, Structure, and Applications of Thin Films of Silicon Monoxide and Titanium Dioxide," *Journal of the American Ceramic Society*, Vol. 33, Dec. 1950, pp. 353-360.

[23]Bradford, A. P., Hass, G., McFarland, M. and Ritter, E., "The Effect of the Substrate Temperature on the Optical Properties of Reactively Evaporated Silicon Oxide Films," *Thin Solid Films*, Vol. 42, 1977, pp.361-367.

[24]*Handbook of Thin Film Technology*, edited by L. I. Maissel and R. Glang, McGraw-Hill, New York, 1970, pp. I-65 – I-73.

[25]Smith, H. R., Kennedy, K., and Boericke, F. S., "Metallurgical Characteristics of Titanium-Alloy Foil Prepared by Electron Beam Evaporation," *Journal of Vacuum Science Technology*, Vol. 7, 1970, pp. 45-48.

[26]Foster, J. S. and Pfiefer, W. H., "Vacuum Deposition of Alloys – Theoretical and Practical Considerations," *Journal of Vacuum Science Technology*, Vol. 9, 1972, pp. 1374-1384.

[27]Nimmagadda, R., Raghuram, A. C. and Bunshah, R. F., "Preparation of Alloy Deposits by Continuous Electron Beam Evaporation from a Single Rod-Fed Source," *Journal of Vacuum Science Technology*, Vol. 9, pp. 1406-1412.

[28]Akers, R. R., Griffing, N., and Buehl, B. C., "A Water-Cooled Nonconsumable Electrode for Vacuum Melting," *Transactions of the International Vacuum Metallurgy Conference*, 1969, p. 357.

[29]Pidgeon, L. M., "Thermal Production of Magnesium," *The Canadian Institute of Mining and Metallurgy*, Vol. 49, 1946, pp. 621-635.

[30]Krueger, J., "Use of Vacuum Techniques in Extractive Metallurgy and Refining of Metals," *Vacuum Metallurgy*, edited by O. Winkler and R. Bakish, Elsevier, New York, 1971, pp. 183-185.

[31]Pfann, W. G., *Zone-Melting*, Wiley, New York, 1958.

[32]*Metals Handbook*, Vol. 8, edited by T. Lyman, American Society of Metals, Metals Park, 1973.

[33]Honig, R. E., *RCA Review*, Vol. 23, 1962, p. 567.

[34]Holland, L., *Vacuum Deposition of Thin Films*, Wiley, New York, 1960, pp. 138-141.

[35]Kelley, K. K., "Free Energies of Vaporization and Vapor Pressure of Inorganic Substances," Bureau of Mines Bulletin 383, U. S. Government Printing Office, 1935.

[36]Reichelt, W. and Mueller, P., *Vakuum-Technologie*, No. 8, 1962.

[37]Drowart, J., "Condensation and Evaporation of Solids," edited by E. Ruther, P. Goldfinger, and J. P. Hirth, Gordon and Breach, Science Publisher, New York, 1964, p. 225.

[38]Schaefer, H., Hoernle, R. Z., *Anorgische Allgemeine Chemile*, 263, 1950, p. 26.

[39]Tombs, N. C. and Welch A. J., Iron Steel Inst., 172, 1952, p. 69.

[40]Hacman, D., Huber W. K., and Retinghaus, G., Ext. Abstr. 14th AVS Symp., 1967, p. 27.

[41]Simons, E. L., "Scientific Foundations of Vacuum Technique," edited by S. Dushman, Wiley, New York, 1962, p. 760.

Effects of Cross Section and Nose Geometry on Slender-Body Supersonic Aerodynamics

G. R. Hutt* and A. J. Howe†
University of Southampton, Hants, England, United Kingdom

Nomenclature

C_D	= drag coefficient
C_L	= lift coefficient
d_B	= cylinder diameter
d_N	= blunt-nose diameter
$Re(d_B)$	= Reynolds number based on cylinder diameter
X_{cp}	= center-of-pressure location aft of nose-afterbody interface
α	= angle of attack
Ψ	= angle of roll

Received Aug. 7, 1987; revision received Oct. 5, 1987.

*Lecturer, Aeronautics and Astronautics Department. Member AIAA.

†Undergraduate Student, Aeronautics and Astronautics Department.

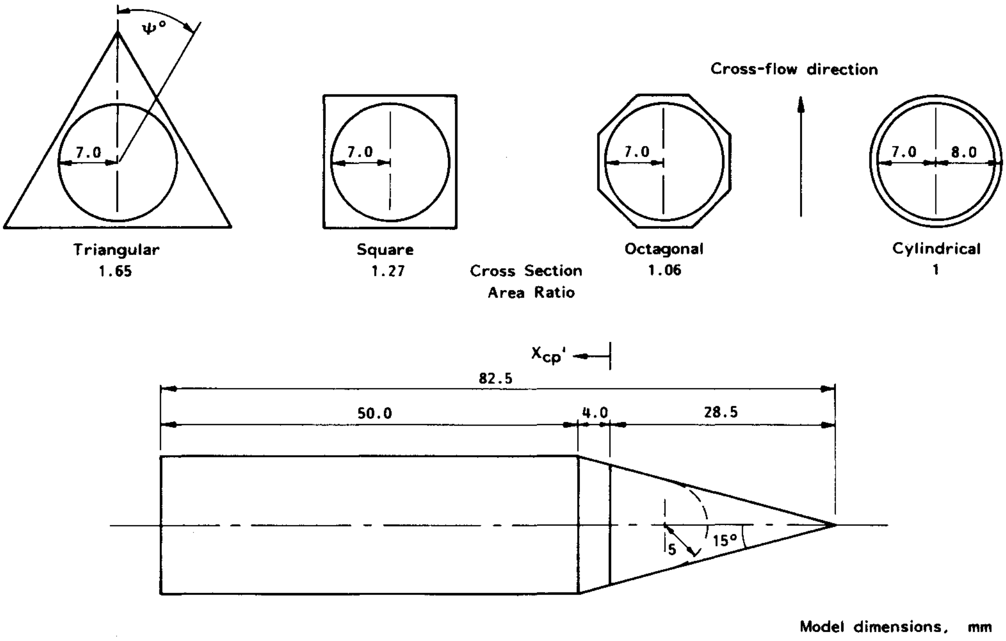

Fig. 1 Schematic of models tested.

Introduction

THE development of higher-performance missiles has stimulated research into noncircular cross sections, e.g., Jackson and Sawyer[1] and Daniel et al.[2] The implications relate to bank-to-turn capability and improved storage capacity for multiple unit packing.

This Note presents details from an experimental program to examine the effect of octagon, square, and triangular cross-section shape, coupled with nose geometry on the supersonic aerodynamics of a family of "slender" shapes. The results presented are static force coefficients C_L, C_D, and center-of-pressure plots as a function of angle of attack and roll angle.

Facility and Models

The experiments were performed in the University of Southampton's closed-circuit induction supersonic wind tunnel. This tunnel provides a flow Mach number of 1.64 for durations of typically 30 s, during which the installed strain-gaged, shrouded sting support traverses 0 deg $\leq \alpha \leq$ 15 deg.

The models tested in the program consisted of forebody/afterbody combinations. The two axisymmetric forebody-nose sections constituted a pointed and blunted 15 deg half-angle cone. The afterbody family comprised circular, octagonal, square, and triangular cross sections. A schematic of the model assembly is shown in Fig. 1. The family reference area S is the cross-section area of the mother circular cylinder afterbody about which the noncircular shapes were based, preserving the 7-mm i.d. for the sting mount. The blunt-nosed forebody has a bluntness ratio of $d_N/d_B = 0.625$, where d_B is the family cylinder diameter. The Reynolds number is $Re(d_B) = 2.4 \times 10^5$.

Results and Discussion

The lift and drag coefficients vs angle of attack for the pointed-cone and blunted-cone family configurations are shown in Figs. 2 and 3. The lift-curve slopes for data $\alpha < 6$ deg are approximately linearly independent of nose shape or afterbody. The flat-bottom cross sections sustain linearity beyond 6 deg, with the most pronounced nonlinearities occurring with the cylinder and octagon afterbodies.

The C_D vs angle-of-attack data shows C_D to be approximately constant to $\alpha = 6$ deg, beyond which

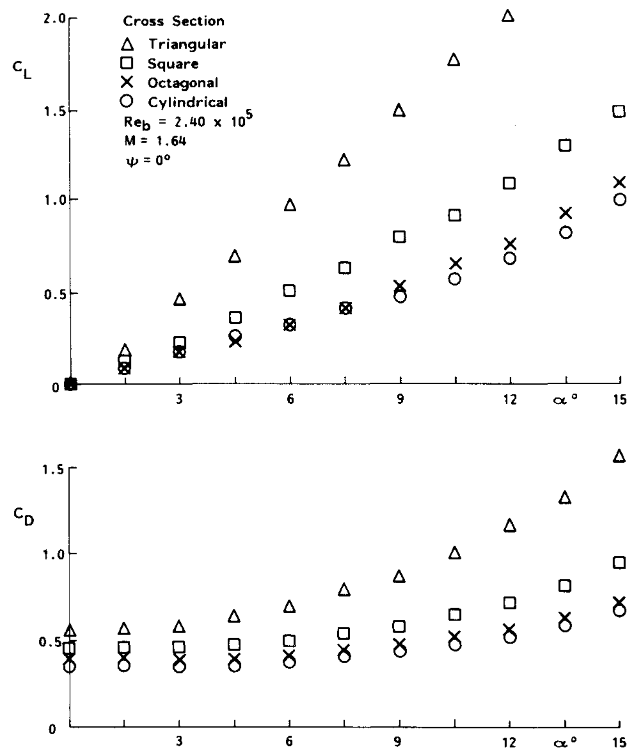

Fig. 2 C_L, C_D vs angle of attack for the pointed-cone nose models.

angle-of-attack-dependent nonlinearities are present, with the most significant nonlinearities being associated with the triangular cross section. The high multisurface octagonal shape is perceived by the flow as being similar to the circular form in that C_L and C_D data are similar. Because of this observation, reduced emphasis is placed on the discussion of the octagon cross-section model data.

The center-of-pressure location as a function of angle of attack, for the cylinder, square, and triangular cross-section models, is shown in Fig. 4. Clearly, at low angles of attack, the nose shape will dominate the pressure distribution. The effect of the blunt nose at near zero angle of attack is to bring the center of pressure forward compared to the pointed-nose configurations. However, at increased angle of attack,

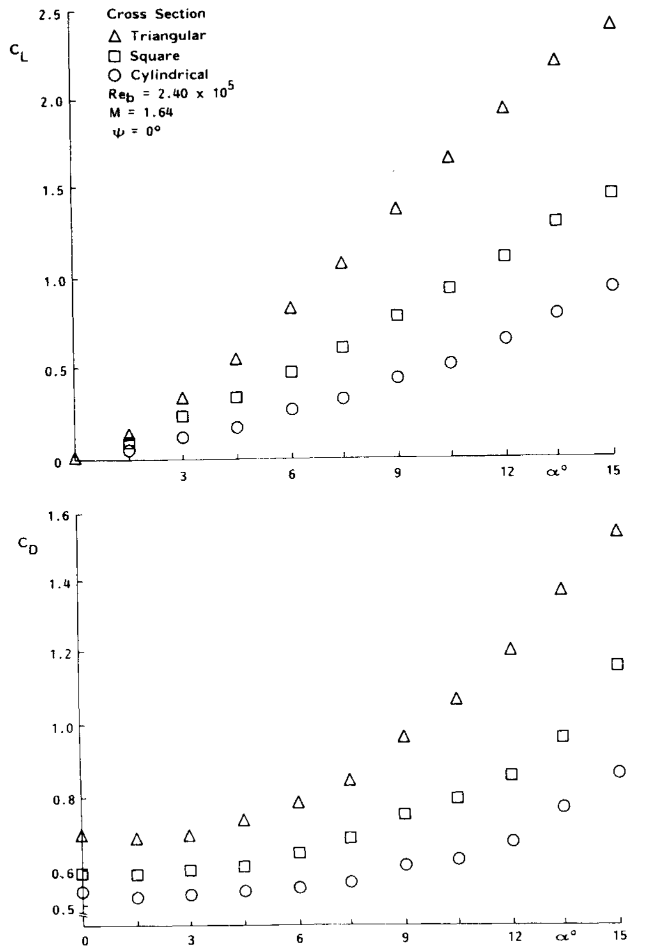

Fig. 3 C_L, C_D vs angle of attack for the blunted-cone nose model.

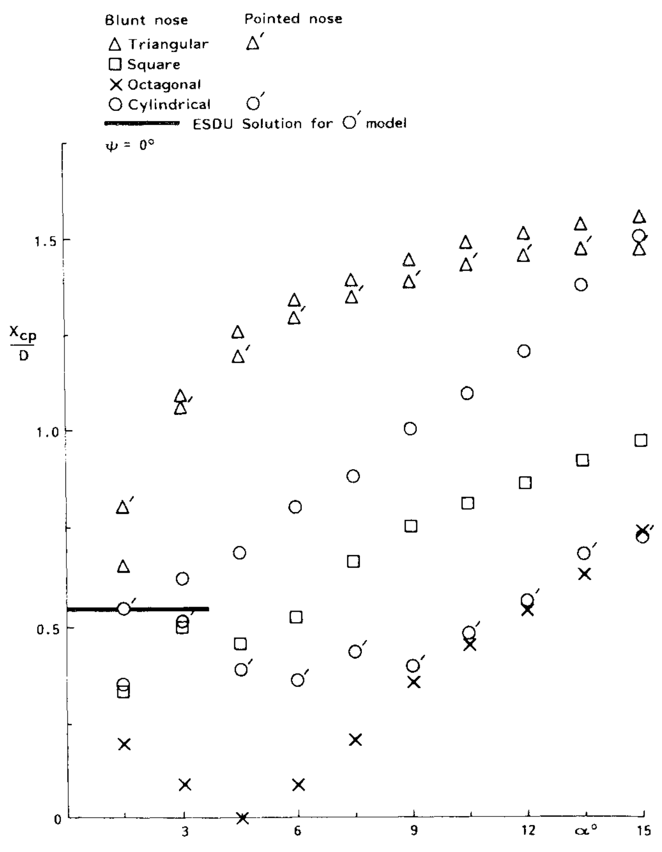

Fig. 4 Center-of-pressure locations vs angle of attack.

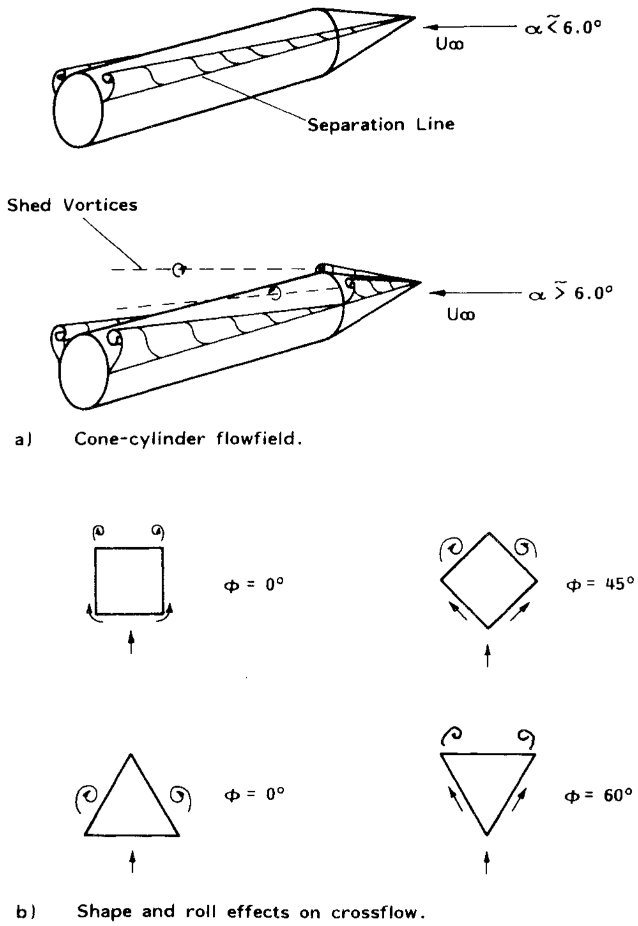

Fig. 5 Leeward surface vortex formation.

$\alpha \geq 3$ deg; the reverse applies, with the cylinder offering the most pronounced difference. The experimental data of the pointed-cone nose cylinder model compare well with the prediction method of ESDU.[3]

The angle-of-attack-dependent trend in center-of-pressure location movement is cross-section-sensitive. The triangular cross-section model attains a more rearward station than the circular cross-section model with a $X_{cp} = f(\alpha)^n$ relationship, where $n < 1$. Unlike the static force coefficient data, the octagon clearly shows different X_{cp} trends than those of the cylinder. Of particular note are the trends in $d(X_{cp}/D)/d\alpha$ with respect to static margin.

The near zero angle-of-attack characteristics are dominated by nose geometry. With increasing angle of attack, the contributions of the exposed afterbody and associated viscous crossflows dominate. For the pointed-cone nose cylinder geometries, the viscous-layer development is postulated as in Fig. 5a, with the separated flow lifting clear of the vehicle for $\alpha > 6$ deg. This is thought to explain the observed $C_L : \alpha$ and $C_D : \alpha$ trends. Surface discontinuities in the crossflow plane serve to modulate the upper surface vortex flow, with the abrupt contour changes acting as separation anchor points, as shown in Fig. 5b. The nature of these cross-section-dependent effects on the viscous crossflows are thought to explain the cross-section-dependent observed trends in C_L, C_D, and X_{cp}.

The roll sensitivity of lift and drag coefficients is summarized, for the square and triangular models, in Fig. 6. The roll sensitivity is increasingly pronounced with angle of attack, and the $\alpha = 15$ deg data are expressed in the dimensionless form $C_L(\Psi)/C_L(\Psi = 0 \text{ deg})$ vs $\Psi/\Psi(\text{form})$, where $\Psi(\text{form})$ is the maximum roll angle from $\Psi = 0$ deg to the nonrepeated orientation of the form; i.e., for the square, $\Psi(\text{form}) = 45$ deg; for the triangle, $\Psi(\text{form}) = 60$ deg. The

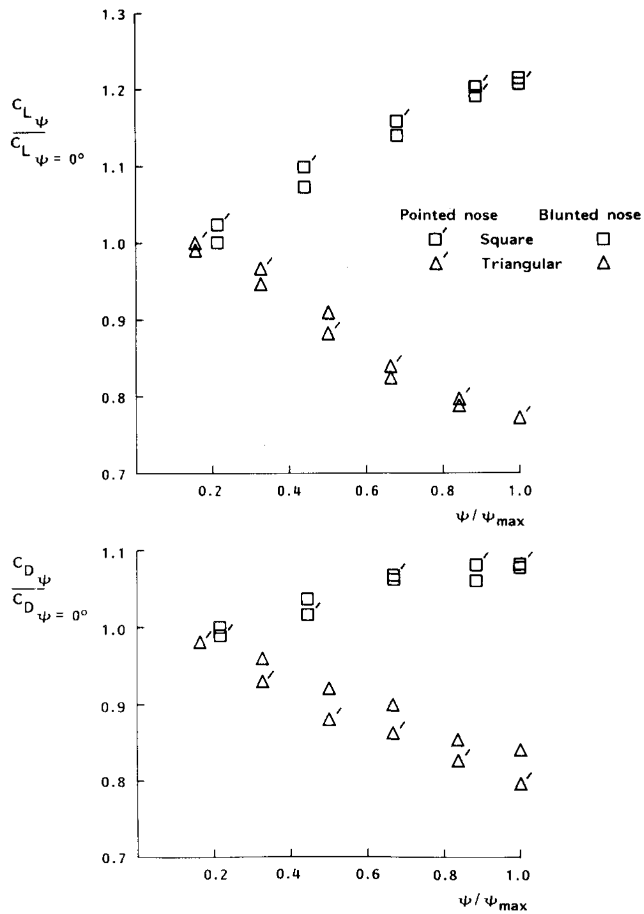

Fig. 6 Roll effect on C_L and C_D, $\alpha = 15$ deg.

most significant feature is that the lift and drag coefficients increase with roll angle for the square model but decrease for the triangular model. At this high angle of attack, the sharp/blunt contrast is minimal, as expected.

The postulated crossflow fields of Fig. 5b, referenced with the roll data, identify two competing influences; namely, windward flow contributions and upper surface vortex formation. Leeward surface vortex formation anchored by a surface discontinuity adjacent to a nonflat leeward surface appear to promote increased lift and drag. This is in agreement with the ogive-nose square cross-section normal-force coefficient transonic/supersonic data of Schneider.[4]

Concluding Remarks

A family of slender geometries of various cross-section shape and nose geometry has been tested in a supersonic wind-tunnel facility. Nose sensitivity coupled with afterbody geometry effects have been identified. The vortex flows present are strongly influenced by the viscous crossflow/cross-section shape interaction. Of the cross sections evaluated, the most favorable cross section for high lift capability at angle of attack is the triangular form. This is thought to be due to early azimuthal separating vortical flow formation adjacent to a near-flat leeward surface.

References

[1]Jackson, C. M. and Sawyer, W. C., "Bodies with Non-circular Cross Sections and Bank-to-Turn Missiles," *Progress in Astronautics and Aeronautics: Tactical Missile Aerodynamics*, Vol. 104, edited by Michael Hemsch and Jack Nielsen, AIAA, New York, 1986.

[2]Daniel, D. C., Lijweski, L. E., and Zollars, G. F., "Experimental Aerodynamic Studies of Missile with Square Cross Sections," AGARD CP 336, Sept. 1982.

[3]Engineering Sciences Data Unit, London, England, Data Sheet Aero 86029, 1986.

[4]Schneider, W., "Experimental Investigation of Bodies with Non-circular Cross Section in Compressible Flow," AGARD CP 336, Sept. 1982.

Notice to Subscribers

We apologize that this issue was mailed to you late. As you may know, AIAA recently relocated its headquarters staff from New York, N.Y. to Washington, D.C., and this has caused some unavoidable disruption of staff operations. We will be able to make up some of the lost time each month and should be back to our normal schedule, with larger issues, in just a few months. In the meanwhile, we appreciate your patience.